

Reviewer 1:

We thank the reviewer for the careful reading of the manuscript and helpful comments. We have revised the manuscript following his/her suggestions as is described below.

Reviewer #1: The manuscript studies the BC deposition and its radiative effect on the snow cover in the northern Tibetan Plateau. Two sets of measurements were used in this study, which included the air samplings of BC particles during 2004-2006 and the ice core drillings of BC deposition during 1986-1994. These data are very interesting and valuable. In addition, two numerical models are used in this study to analyze the data, including; a global chemical transportation model (MOZART-4) and a radiative transfer model (SNICAR). Their analysis shows that there is a high peak of BC deposition at Muztagh Ata in Northern Tibetan Plateau during 1991-1992 (about 3-4 times higher than other years), caused by the large Kuwait fires at the end of the first Gulf War in 1991. This result suggests that the upward BC emissions had important impacts on this remote site located in Northern Tibetan Plateau. The radiative effect calculated by the radiative Only one month sampling of PM_{2.5} was conducted in this study, which cannot view the current status of atmospheric fine PM_{2.5}. At least four seasons are commonly required in a typical PM_{2.5} study. transfer model (SNICAR) shows that a significant increase for the snow melting in Northern Tibetan Plateau due to this fire event. This study is suitable for the scientific scope of ACP, and can be accepted for the publication in ACP. However, there are some minor comments, which should be addressed in the revised version;

Comments; (1) The Authors define 4 BC source regions, which could have important impacts on the BC deposition at the remote site located in Northern Tibetan Plateau. They should make more detailed description for the definition of these 4 regions.

Response: To address the reviewer's comments, we define the 4 sources regions with a detailed description. The corresponding revision can be found from the line 414 to 422. We also plotted the topography of the study region as shown in Fig.1.

(2) The Authors have detailed description for the ice core drill measurements. However, the description of TSP is rather too simple. More descriptions of the TSP should be required.

Response: According to the suggestion, we added the information of the samplers of TSP, including sampling flow rates, power of device and the identification of valid samples from the line 163 to 172. The description of ice core drill measurements in section 2.2 has been revised correspondingly.

(3) The quality of Fig. 6 should be improved. The labels are too small.

Response: Fig.6 has been improved as request.

(4) There are some English typos. For example, in the line 297, Page 9, “In order to the effect of the huge Kuwait fires on the BC ice core deposition” should be “In order to study the effect of the huge Kuwait fires on the BC ice core deposition”

Response: Corrected. We’ve also checked other typos and make corrections in the revised version.

Reviewer 2:

We thank the reviewer for the careful reading of the manuscript and helpful comments. We have revised the manuscript following his/her suggestions as is described below.

Reviewer #2: This article investigate the large Kuwait fires on BC deposition on the ice core at Muztagh Ata Mountain, Northern Tibetan Plateau and the related radiative forcing. It has excellent scientific point and is meaningful for the current Tibetan Plateau experiments. I strongly suggest the acceptance and quick publication of the article. Following are some comments and suggestions for the paper:

(1) In Fig.1, the topography should be plotted to illustrate the plateau characteristics.

Response: The topography of Fig.1 has been updated.

(2) In Fig.2, the BC measurements were much lower during Apr to May of 2004, and sharply increased on Jun, while the model results were very flat, the author should give some explanations.

Response: To address the reviewer’s comment, we make explanation that the difference between the measured and the modeled BC concentrations during the spring of 2004 is due to the uncertainties of the emissions, simulated meteorological parameter and the low horizontal resolution, which lead to

difference of topography between the model and actual situation. These explanations can be added from line 309 to 320.

(3) I suggest the author made more discussion on the possible impact of the change of ice on regional climate, such as the flood, the drought in china.

Response: Thanks for the constructive suggestion from reviewer. We've added discussion from the line 516-542.

Black carbon (BC) in North Tibetan Mountain; Effect of Kuwait fires on glacier

Jiamao Zhou^{1,6}, Xuexi Tie^{1,2}, Baiqing Xu³, Shuyu Zhao¹, Mo Wang³, Guohui Li¹,
Ting Zhang¹, Zhuzi Zhao^{1,7}, Suixin Liu¹, Song Yang³, Luyu Chang^{4,5}, Junji Cao¹

¹KLACP, SKLLQG, Institute of Earth Environment, Chinese Academy of Sciences, Xi'an 710061, China

²Center for Excellence in Urban Atmospheric Environment, Institute of Urban Environment, Chinese Academy of Sciences, Xiamen 361021, China

³Key Laboratory of Tibetan Environment Changes and Land Surface Processes, Institute of Tibetan Plateau Research, Chinese Academy of Sciences, Beijing 100101, China

⁴Shanghai Meteorological Service, Shanghai, 200030, China

⁵Shanghai Key Laboratory of Meteorology and Health, Shanghai, 200030, China

⁶ University of Chinese Academy of Sciences, Beijing 100049, China

⁷[School of Chemistry & Environmental Engineering, Jiangsu University of Technology](#)

Correspondence to: Xue Xi Tie (tiexx@ieecas.cn) or Baiqing Xu (baiqing@itpcas.ac.cn)

带格式的：突出显示

带格式的：上标，突出显示

带格式的：突出显示

带格式的：上标

带格式的：突出显示

带格式的：上标，突出显示

带格式的：突出显示

带格式的：段落间距段前：0.5 行

带格式的：段落间距段前：0.8 行

带格式的：上标

带格式的：行距：1.5 倍行距，不对齐到网格

带格式的：字体：（默认）Times New Roman,（中文）+中文正文, 10磅, 字体颜色：文字 1

24 **Abstract.** The BC deposition on the ice core at Muztagh Ata Mountain, Northern
25 Tibetan Plateau was analyzed. Two sets of measurements were used in this study,
26 which included the air samplings of BC particles during 2004-2006 and the ice core
27 drillings of BC deposition during 1986-1994. Two numerical models were used to
28 analyze the measured data. A global chemical transportation model (MOZART-4)
29 was used to analyze the BC transport from the source regions, and a radiative transfer
30 model (SNICAR) was used to study the effect of BC on snow albedo. The results
31 show that during 1991-1992, there was a strong spike of the BC deposition at
32 Muztagh Ata, suggesting that there was an unusual emission in the upward region
33 during this period. This high peak of BC deposition was investigated by using the
34 global chemical transportation model (MOZART-4). The analysis indicated that the
35 emissions from large Kuwait fires at the end of the first Gulf War in 1991 caused this
36 high peak of the BC concentrations and deposition (about 3-4 times higher than other
37 years) at the Muztagh Ata Mountain, suggesting that the upward BC emissions had
38 important impacts on this remote site located in Northern Tibetan Plateau. Thus, there
39 is a need to quantitatively estimate the effect of surrounding emissions on the BC
40 concentrations in the northern Tibetan Plateau. In this study, a sensitive study with 4
41 individual BC emission regions (Central Asia, Europe, Persian Gulf, and South Asia)
42 was conducted by using the MOZART-4 model. The result suggests that during the
43 “normal period” (non Kuwait Fires), the largest effect was due to the Central Asia
44 source (44%) during Indian monsoon period, while during non-monsoon period, the
45 largest effect was due to the South Asia source (34%). The increase of radiative
46 forcing increase (RFI) due to the deposition of BC on snow was estimated by using
47 the radiative transfer model (SNICAR). The results shows that under the fresh snow
48 assumption, the estimated increase of RFI ranged from 0.2 W m^{-2} to 2.5 W m^{-2} , while
49 under the aged snow assumption, the estimated increase of RFI ranged from 0.9 W
50 m^{-2} to 5.7 W m^{-2} . During the Kuwait fires period, the RFI values increased about 2-5
51 times higher than the “normal period”, suggesting a significant increase for the snow
52 melting in Northern Tibetan Plateau due to this fire event. This result suggests that the
53 variability of BC deposition at the Muztagh Ata Mountain provides useful information
54 to study the effect of the upward BC emissions on environmental and climate issues in
55 the Northern Tibetan Plateau. The radiative effect of BC deposition on the snow
56 melting provides important information regarding the water resources in the region.—
57 —

带格式的：字体：小四

带格式的：定义网格后自动调整
右缩进，调整中文与西文文字的间
距，调整中文与数字的间距

58 | **Key Words; Northern Tibetan glaciers, BC deposition, MOZART model**

59

带格式的：定义网格后不调整右缩进，不调整西文与中文之间的空格，不调整中文和数字之间的空格，不对齐到网格

1 Introduction

Black carbon (BC) particles emitted from combustion are considered as an important air pollutant, as they ~~have direct effect~~ ~~change the radiative balance of the atmosphere~~ ~~directly~~ by absorbing and scattering solar radiation, and indirect ~~effect~~ ~~by~~ ~~the~~ ~~change of cloud microphysical processes~~ ~~the microphysical process of cloud~~ (acting as ice nuclei) and ~~efficiency of~~ precipitation ~~efficiency~~ (acting as cloud condensation nuclei) (Ramanathan et al., 2001). Albedo changes induced by strongly light absorbing component by deposited on the surface of snow and ice are ~~the key key~~ parameters ~~to determine govern the~~ radiative forcing and accelerate melting (Holben et al., 1998; Hansen and Nazarenko, 2004). ~~Due to the strong regional to local distribution of BC,~~ ~~These important~~ properties make BC as a key topic related with ~~climate change but~~ are not well understood ~~due to the very different inhomogeneous spatial and temporal distribution of BC, especially in remote areas, particularly in remote regions,~~ such as the Tibetan Plateau.

BC particles can deposit and preserve in the ice by the progress of post-deposition on the glaciers and ice sheets. Retrieved ice cores from remote mountain glaciers and ice sheets provide useful information of the historical BC aerosol emissions and synchronous meteorology conditions. Previous studies on records of carbonaceous aerosols show that the emissions of fossil fuel combustion from Central Europe had significant impact on the glacier in the Swiss Alps (Lavanchy et al., 1999). ~~Bisiaux et al., (2012), analyzed two ice cores drilled in Antarctica and found that the ice core records of BC deposition reflected the change of atmospheric BC emission, distribution and transport in Southern Hemisphere. By ice cores drilled from Antarctica suggest that the Southern Hemisphere biomass burning were strongly influenced by continental hydrology (Bisiaux et al., 2012), using an ice core in Greenland, (McConnell et al. (2007), differentiated the BC emissions from industrial activities and forest fires, are differentiated, (using an ice core in Greenland, McConnell et al. (2007), differentiated t.~~ These researches indicate that BC records in history are important and practicable method to investigate the regional aerosol transport and emission variations.

In this study, the ice core BC at Muztagh Ata, Northern Tibetan Plateau is analyzed.

带格式的: 字体: 小四

带格式的: 字体: 小四

带格式的: 字体: 小四

带格式的: 字体: 小四

带格式的: 字体: 小四

带格式的: 字体: 小四

带格式的: 字体: 小四

带格式的: 字体: 小四

带格式的: 字体: 小四

带格式的: 字体: 小四

带格式的: 字体: 小四

带格式的: 字体: 小四

带格式的: 字体: 小四

带格式的: 字体: 小四

带格式的: 字体: 小四

带格式的: 非突出显示

带格式的: 字体: 小四

带格式的: 非突出显示

带格式的: 字体: 小四

带格式的: 字体: 小四

带格式的: 非突出显示

带格式的: 非突出显示

带格式的: 非突出显示

带格式的: 字体: 小四

带格式的: 字体: 小四

带格式的: 字体: 小四

带格式的: 字体: 小四

带格式的: 非突出显示

带格式的: 非突出显示

带格式的: 字体: 小四

带格式的: 字体: 小四

带格式的: 字体: 小四

带格式的: 非突出显示

带格式的: 字体: 小四

带格式的: 字体: 小四

带格式的: 非突出显示

带格式的: 字体: 小四

带格式的: 非突出显示

带格式的: 字体: 小四

带格式的: 非突出显示

带格式的: 非突出显示

带格式的: 非突出显示

带格式的: 字体: 小四

带格式的: 字体: 小四

93 Identification the source regions, which have important impact on BC deposition at
94 Muztagh Ata is very important scientific issue, because of its location. In particularly,
95 there was a strong spike of the BC deposition during 1992-1993 at Muztagh Ata (as
96 shown in the following text), reflecting that there was unusual emission in the upward
97 region from Muztagh Ata. This strong spike of the ice core BC was about 3-4 times
98 higher than other years, producing important effects on climate and hydrological cycle.
99 As a result, the study of the sources of BC, which affect the ice core BC in this
100 location, needs to be carefully studied. Muztagh Ata locates in the east of Pamir and
101 the north of Tibetan Plateau. The ice core data provides important information for
102 atmospheric circulation and climate change in Asia (An et al., 2001). Moreover, the
103 climate in Muztagh Ata is very sensitive to solar warming mechanisms because it has
104 a large snow cover in the region, resulting in important impacts on the hydrological
105 cycle of the continent by enhancing glacier melt.

带格式的: 字体: 小四
带格式的: 字体: 小四

106
107 The BC sources which contribute the BC deposition in Tibetan Plateau have been
108 previously studied. Their results show that BC deposited on glaciers ~~in of~~ the Pamir
109 Mountains was ~~emitted/originated~~ from Europe, Middle East and central Asia (Liu
110 et al., 2008; Xu et al., 2009a; Wang et al., 2015b), whereas BC ~~deposited/deposition on~~
111 ~~glaciers on snow and ice~~ over the Himalayas and southeastern Tibetan Plateau was
112 mainly affected by the western upward regions in winter. During the Indian summer
113 monsoon season, they were mainly affected by the BC sources in Indian region (Ming
114 et al., 2008; Xu et al., 2009b; Kaspari et al., 2011; Wang et al., 2015a). However, at
115 present, the effects of the transport pathways and individual contributions of BC
116 sources to the Muztagh Ata region have not been carefully studied. Because the
117 radiative forcing caused by BC in snow and ice between different regions is very
118 different, depending upon the emitting intensities, ocean-land distributions,
119 topography, regional atmospheric circulations, and other factors, detailed study on the
120 source contributions to the region as well as the climate effect are needed to carefully
121 study this important region.

带格式的: 字体: 小四
带格式的: 非突出显示
带格式的: 字体: 小四
带格式的: 非突出显示
带格式的: 字体: 小四
带格式的: 非突出显示
带格式的: 字体: 小四
带格式的: 字体: 小四
带格式的: 字体: 小四
带格式的: 非突出显示
带格式的: 字体: 小四
带格式的: 非突出显示
带格式的: 字体: 小四
带格式的: 字体: 小四
带格式的: 字体: 小四

122
123 Both the ice core deposition measurements at Muztagh Ata and a global chemical
124 model (MOZART-4; Model for Ozone and Related chemical Tracers, version 4) are
125 used in this study. To better evaluate the model performance, the air samples of BC
126 particles during ~~2004-2006~~1986-1994, were also analyzed. The global chemical

带格式的: 字体: 小四, 突出显示
带格式的: 字体: 小四

127 transport model (MOZART-4) was used to analyze the long-term trend in the early
128 90s of the observed BC deposition and to quantify the individual contribution of
129 different BC sources to the deposition on the snow cover. The modeled temporal
130 variations and magnitude of the BC concentrations in the atmosphere and snow were
131 compared to observations. Finally, a radiative transfer model (SNICAR) was used to
132 study the effect of BC on snow albedo, radiative forcing, and runoff changes induced
133 by the BC deposition on the Muztagh Ata snow.

134

135 **2 Methodologies**

136 **2.1 Sampling Sites**

137 Muztagh Ata Mountain is located in the north side of Tibetan Plateau. Both
138 atmospheric sampling and ice core drilling BC were conducted at the Muztagh Ata
139 site. The atmospheric sampling BC (38°17.30'N, 75°01.38'E) was conducted [by-in](#)
140 the Cold and Arid Regions Environmental and Engineering Institute, Chinese
141 Academy of Sciences, at a 4500 m above sea level (a.s.l.). A 170.4 m ice core (9.5 cm
142 in diameter) was drilled during the summer season in 2012 from Kuokuosele (KKSL)
143 Glacier of Muztagh Ata (38°11'N, 75°11'E, 5700 m a.s.l.), which was conducted by
144 the Institute of Tibetan Plateau Research, Chinese Academy of Sciences. Because the
145 site is surrounded by several important BC source regions, this measurement site is
146 suitable to investigate the effect of BC emissions on north part Tibetan Plateau, which
147 plays important roles for global climate and hydrology (see Fig. 1).

148

149 The average annual temperature at the peak of the mountain is approximately -20°C.
150 Because the numerous high mountains block the warm and humid air currents from
151 Indian and Pacific Ocean, the climate in this area is relatively dry. The averaged
152 annual precipitation is less than 200 mm, which is mainly snow to form perennial
153 glaciers. There are 128 modern glaciers and on average about 377 square kilometers.
154 The prevailing winds in this region are usually westerly jet stream. Previous studies
155 suggested that there was very small effect by local sources, and the aerosol pollutions
156 were originated mainly from the west by mid- and long-range transport. During
157 summer, the South Asia monsoon had also important effect on the transport of BC
158 particles from India (Liu et al., 2008; Wu et al., 2008; Zhao et al., 2011; Wang et al.,

带格式的：字体：小四

159 2015b).

带格式的：字体：小四

160

161 2.2 Measurements

162

163 During the period from December 5, 2003 to February 17, 2006, **Eighty-one valid**

带格式的：字体：小四，突出显示

164 **total suspended aerosol particle (TSP) and BC samples** were obtained **with**

165 **custom-made samplers at flow rates of 16 l min⁻¹**. The measurements were conducted

带格式的：字体：小四，上标，突出显示

166 under very difficult environmental conditions, because of its high mountain location.

带格式的：字体：小四，突出显示

167 **The sampler power was supplied by solar energy and a storage battery.** ~~The sample~~

带格式的：字体：小四

168 ~~numbers for spring, summer, autumn, and winter was 19, 21, 14, 27, respectively.~~

带格式的：字体：小四，突出显示

带格式的：字体：小四

169 Each sample was collected over one week and on 15 mm Whatman quartz microfibre

170 filter (QM/A, Whatman LTD, Maidstone, UK), which was pre-combusted at 800°C

带格式的：字体：小四，(国际) Times New Roman

171 for 3 hours to remove the potential carbon disturbance. **The sample was identified as**

带格式的：字体：小四，突出显示

172 **valid when its sampling standard volume was greater than 30 m³**. **As a result, the valid**

带格式的：字体：小四，上标，突出显示

173 **sample numbers for spring, summer, autumn, and winter were 19, 21, 14, and 27,**

带格式的：字体：小四，突出显示

174 **respectively.**

带格式的：字体：小四

175

176 For the ice core measurement, a 170.4 m ice core (9.5 cm in diameter) was drilled

177 during the summer season in 2012 from Kuokuosele (KKSL) Glacier of Muztagh Ata

178 (38°11'N, 75°11'E, 5700 m a.s.l.), which is close to the BC air sampling site. **A**

179 **stainless steel scalpel that pre-cleaned at -5°C in a class 100 laminar flow bench was**

180 **used to remove. A 3 mm outer layer of the ice sections core was removed with a**

带格式的：字体：小四

带格式的：字体：小四

181 **pre-cleaned stainless steel scalpel at -5°C in a class 100 laminar flow bench to**

带格式的：字体：小四，(国际) Times New Roman

182 **eliminate/exclude the pollutant/contamination that might be mixed in/have occurred**

带格式的：字体：小四

带格式的：字体：小四

183 during drilling, transport, and storage. ~~The inner section for BC analysis was sealed in~~

带格式的：字体：小四

184 ~~a 50 ml polypropylene vial (BD Falcon, cat. no. 358206).~~ The ice core dating and

185 calculation of BC deposition fluxes were provided by Institute of Tibetan Plateau

186 Research, Chinese Academy of Science. The detailed method for the measurement of

187 BC deposition is shown by Xu et al. (2009a).

带格式的：字体：小四

带格式的：字体：小四

188

189 2.3 Measurements and Analytical methods

带格式的：字体：Times New Roman，小四

190

191 The elemental carbon (EC, which is proxy to BC in this study) analyses for

带格式的：字体：小四

带格式的：字体：小四，非加粗，字体颜色：自动设置

192 atmospheric filters (**TSP samples**) were carried out by using Desert Research Institute

带格式的：字体：小四

193 (DRI) Model 2001 carbon analyzer (Atmoslytic Inc., Calabasas, CA, USA) with
194 IMPROVE (Interagency Monitoring of PROtected Visual Environments)
195 thermal/optical reflectance (TOR) protocol (Chow et al., 1993; Chow et al., 2004). A
196 0.526 cm² punch of a quartz filter sample was heated in a stepwise manner to obtain
197 data for three elemental carbon (EC) fractions ~~(EC1, EC2, and EC3 in a 2%~~
198 ~~oxygen/98% helium atmosphere at 580, 740, and 840 °C.~~ At the same time, OP
199 (pyrolyzed carbon) was produced at <580 °C in the inert atmosphere which decreases
200 the reflected light to correct for charred OC. Total EC is the sum of the three EC
201 fractions minus OP. More details and QAQC (Quality Assurance and Quality Control)
202 are shown by Cao et al. (2003) and Cao et al., (2009).

带格式的: 字体: 小四

带格式的: 字体: 小四

带格式的: 字体: 小四, (国际)
Times New Roman

带格式的: 字体: 小四

带格式的: 字体: 小四, (国际)
Times New Roman

带格式的: 字体: 小四

带格式的: 字体: 小四

带格式的: 字体: 小四

带格式的: 字体: 小四

带格式的: 字体: 小四

带格式的: 字体: 小四

带格式的: 字体: 小四

带格式的: 字体: 小四

带格式的: 字体: 小四

带格式的: 非突出显示

带格式的: 字体: 小四

带格式的: 非突出显示

带格式的: 字体: 小四

带格式的: 非突出显示

带格式的: 字体: 小四

带格式的: 字体: 小四

带格式的: 字体: 小四

带格式的: 非突出显示

带格式的: 字体: 小四

带格式的: 非突出显示

带格式的: 字体: 小四

带格式的: 非突出显示

带格式的: 字体: 小四

带格式的: 字体: 小四

带格式的: 字体: 小四

带格式的: 字体: 小四

带格式的: 字体: 小四

带格式的: 字体: 小四

带格式的: 字体: 小四

带格式的: 字体: 小四

带格式的: 字体: 小四

带格式的: 字体: 小四

带格式的: 字体: 小四

带格式的: 字体: 小四

带格式的: 字体: 小四

带格式的: 字体: 小四

203
204 The rBC (refractory black carbon), which is used instead of BC for measurements
205 derived from incandescence methods (Petzold et al., 2013), was analyzed at Institute
206 of Tibetan Plateau Research, Chinese Academy of Sciences by using a Single Particle
207 Soot Photometer (SP2) coupled with an ultrasonic nebulization system (CETAC
208 UT5000). ~~The laser induced incandescence was used to measure the~~ The mass of
209 rBC ~~in of~~ individual particles ~~were measured by using a laser-induced incandescence~~
210 (Schwarz et al., 2006). The incandescence signal can be converted to rBC mass which
211 is detected by photomultiplier tube detectors. ~~Previous studies has~~ This analytical
212 ~~method was previously successfully~~ applied ~~this analytical method to~~ ice cores by
213 ~~several studies/researches~~ (McConnell et al., 2007; Kaspari et al., 2011; Bisiaux et al.,
214 2012). Detailed description on the SP2 analytical process and calibration procedures
215 can be found in (Wendl et al., 2014) and (Wang et al., 2015b).

216
217 Although the differences in the two analytical techniques (Wang et al., 2015b) in
218 order to facilitate the discussions, they are uniformly referred to as black carbon (BC)
219 in our study since both of them are materials share some of the characteristics of BC
220 with its light-absorbing properties (Petzold et al., 2013).

222 2.4 Global chemistry transport model / MOZART-4

223
224 The model used in this study is MOZART-4 (Model for Ozone and Related chemical
225 Tracers, version 4). The model is an offline global chemical transport model for the
226 troposphere developed jointly by the National Center for Atmospheric Research

227 (NCAR), the Geophysical Fluid Dynamics Laboratory (GFDL), and the Max Planck
228 Institute for Meteorology (MPI-Met). The detailed model description and model
229 evaluated can be found in [Emmons et al. \(2010\)](#). The aerosol modules was developed
230 by [Tie et al. \(2005\)](#). This model have been developed and used to quantify the global
231 budget of trace gases and aerosol particles, and to study their atmospheric transport,
232 chemical transformations and removal ([Emmons et al., 2010](#); [Chang et al., 2016](#)).
233 The model is built base on the framework of the Model of Atmospheric Transport and
234 Chemistry (MATCH) ([Rasch et al., 1997](#)). Convective mass fluxes are diagnosed by
235 using the shallow and mid-level convective transport formulation of Hack ([Hack,](#)
236 [1994](#)) and deep convection scheme ([Zhang and McFarlane, 1995](#)). Vertical diffusion
237 within the boundary layer is built on the parameterization by [Holtslag and Boville](#)
238 ([1993](#)). Advective transport scheme used the flux form semi-Lagrangian transport
239 algorithm ([Lin and Rood, 1996](#)). The wet deposition includes in-cloud as well as
240 below-cloud scavenging developed by [Brasseur et al. \(1998\)](#) is taken into
241 MOZART-4. Details of the chemical solver scheme can be found in the Auxiliary
242 Material ([Kinnison et al., 2007](#)).

243
244 In the present study, the model includes 85 gas-phase species, 12 bulk aerosol
245 compounds and approximately 200 reactions. The horizontal resolution of this study
246 is $1.9^{\circ} \times 2.5^{\circ}$ with 56 hybrid sigma-pressure vertical levels from the surface to
247 approximately 2 hPa. The meteorological initial and boundary conditions are down
248 load from NCAR Community Data Portal (CDP), using National Centers for
249 Environmental Prediction (NCEP) meteorology. The model transport of this study is
250 driven by the Modern-Era Retrospective-analysis for Research and Applications
251 (MERRA) 6-hour reanalysis data with a $1.9^{\circ} \times 2.5^{\circ}$ grid provided by National
252 Aeronautics and Space Administration (NASA).

253
254 The BC emission inventory used in this global model is based on the simulation of
255 the POET (Precursors of Ozone and their Effects in the Troposphere) database from
256 1997 to 2007 and the data of BC emission inventory including fossil fuel and biofuel
257 combustion from a previous study ([Bond et al., 2004](#); [Bond et al., 2007](#)). Figure 2
258 illustrates the updated 21-year average global BC emissions from 1986 to 2006. There
259 are two types of black carbon particles in MOZART-4, hydrophobic and hydrophilic
260 particles. Hydrophobic particles are directly emitted from the sources, and are

带格式的: 字体: 小四

带格式的: 字体: 小四

带格式的: 字体: 小四

带格式的: 字体: 小四

带格式的: 字体: 小四

带格式的: 字体: 小四

带格式的: 字体: 小四

带格式的: 字体: 小四

带格式的: 字体: 小四

带格式的: 字体: 小四

带格式的: 字体: 小四

带格式的: 字体: 小四

带格式的: 字体: 小四

带格式的: 字体: 小四

带格式的: 字体: 小四

带格式的: 字体: 小四

带格式的: 字体: 小四

带格式的: 字体: 小四

带格式的: 字体: 小四

带格式的: 字体: 小四

带格式的: 字体: 小四

带格式的: 字体: 小四

converted to hydrophilic in the atmosphere (Hagen et al., 1992; Liousse et al., 1993; Parungo et al., 1994), with a rate constant of $7.1 \times 10^{-6}/s$ (Cooke and Wilson, 1996).

2.5 BC deposition estimation

In order to compare to the measured ice core BC deposition at the Muztagh Ata Mountain, the BC deposition flux is calculated in this study. In the estimation, the calculated atmospheric BC concentrations and precipitation data obtained from China Meteorological Data Service Center were compiled and evaluated. In addition, annual BC deposition parameters and deposition flux calculation methods were described in other studies (Jurado et al., 2008; Yasunari et al., 2010; Fang et al., 2015; Li et al., 2017). In brief, deposition fluxes are calculated by the following equations:

$$F_{DD} = 10^{-4} v_D C_{BC} t$$

(1)

$$F_{WD} = 10^{-7} p_0 W_p C_{BC}$$

(2)

$$F_{BC} = F_{DD} + F_{WD}$$

(3)

where 10^{-4} and 10^{-7} are unit conversion factors; F_{DD} and F_{WD} are the annual dry and wet deposition ($ng\ cm^{-2}$), respectively; the total BC deposition flux (F_{BC}) ($ng\ cm^{-2}$) is the sum of F_{DD} and F_{WD} ; where v_D ($m\ s^{-1}$) is the dry deposition velocity of black carbon; t is total estimation time for one year (s); p_0 is the annual precipitation rate (mm); W_p is the particle washout ratio (dimensionless); and C_{BC} is the annual atmospheric BC concentrations at Muztagh Ata Mountain ($ng\ m^{-3}$). There are large differences in estimates on v_D and W_p (Jurado et al., 2005; Jurado et al., 2008; Yasunari et al., 2013). A fixed small dry deposition velocity of $1.0 \times 10^{-4}\ m\ s^{-1}$ onto snow was adopted (Yasunari et al., 2010; Nair et al., 2013) and the corresponding estimation values are likely to represent a lower bound for BC dry deposition in this area. Particle washout ratio W_p is assumed to be a constant and equal to 2×10^5 which has been adopted in many modeling exercises and fits well with field measurements

带格式的: 字体: 小四

带格式的

带格式的: 字体: 小四

带格式的: 字体: 小四

带格式的: 字体: 小四

带格式的

带格式的: 字体: 小四

带格式的

带格式的

带格式的

带格式的

带格式的

带格式的

带格式的

294 (Mackay et al., 1986; Jurado et al., 2005; Fang et al., 2015; Li et al., 2017).

带格式的: 字体: 小四

带格式的: 字体: 小四

295 3 Results and discussion

296 3.1 Model evaluation and compared to observation

297

298 In order to better understand the variation, characteristics, and source contributions of
299 the BC concentrations at Muztagh Ata Mountain, model sensitive studies using
300 MOZART-4 were conducted in this study. Firstly, the model was evaluated by
301 comparing the observed monthly BC concentrations with the calculated monthly BC
302 concentrations during January 2004 to February 2006. As shown in Fig 3a, the
303 simulated BC concentrations had a similar magnitude of measured BC concentrations,
304 with mean values of 62.4 ng m^{-3} and 56.5 ng m^{-3} for the calculation and measurement,
305 respectively. There was also evident that the measured variability of BC was captured
306 by the calculation. For example, the calculated variability was comparable to the
307 measured result between July 2014 and Oct. 2015. However, some differences were
308 also noticeable. For example, the calculated BC concentration was overestimated in
309 the spring and winter of 2004 and underestimated in the winter of 2006. Because the
310 measured site locates in a “clean” region of BC emission, the BC particles were
311 mostly transported from long-distance of the upwind regions. There were uncertainty
312 related to the emissions and simulated meteorological parameters (wind speeds, wind
313 directions, etc.). As a result, it caused the discrepancy between calculated and
314 measured BC concentrations at the Muztagh Ata Mountain. There was another reason
315 may cause the difficulty of the calculation. The horizontal resolution of the global
316 model is relatively low ($1.9^\circ \times 2.5^\circ$ in this study), which is unable to reproduce some
317 detailed variability in the simulation. However, the overall features of the measured
318 BC concentrations were reproduced by the model, such as the magnitude and seasonal
319 variability (see Fig. 3b), suggesting that the model is capable to study long-range
320 transport from BC source regions to the remote site.

带格式的: 字体: 小四, 突出显示

带格式的: 字体: 小四

带格式的: 字体: 小四, 突出显示

带格式的: 字体: 小四

321

322 The simulated seasonal variation shows in Fig 3b. The result shows that calculated
323 seasonal variation was generally agreed with the measured variation, except the value
324 in spring. According to the analysis of the source contribution (shown in Section 3.3),
325 the BC emission in South Asia has significant contributions to the BC concentrations

326 at Muztagh Ata during non-summer season which accounted for average 31~60% in
327 spring and few contributions in summer season. The overestimated BC concentrations
328 may due to the fact that the model overestimated the pollutant transportation from the
329 emission sources to sampling site crossing the high mountains of Tibet Plateau, which
330 act as a wall to block the transportation from the BC emission in South Asia to the
331 sampling area (Zhao et al., 2013).

带格式的: 字体: 小四

带格式的: 字体: 小四

333 **3.2 Long-term Ice core measurement and possible effect of Kuwait fire event**

334
335 In addition to the atmospheric sampling of BC measurement, there is a long-term ice
336 cores measurement of BC at the Muztagh Ata Mountain. This long-term measurement
337 represents a valuable data to show the long-term trend and inter-annual variability. Ice
338 core records obtained at Muztagh Ata Mountain are irreplaceable when evaluating
339 contemporary atmospheric or snow BC concentration variations. A long-term ice-core
340 measurement (from 1940 to 2010) was provided by Xu et al. at Muztagh Ata
341 Mountain. Their results showed that the ice core BC concentrations were between
342 0.30 and 39.54 ng g⁻¹ from 1940 to 2010, with an average value of 7.22 ng g⁻¹. The
343 BC deposition fluxes were between 9.96 and 909.88 ng cm⁻², with an average of
344 184.18 ng cm⁻². It is interesting to note that both BC concentration and BC deposition
345 of ice core showed a sharply increase in 1992, which was about five times higher than
346 the average mean value as shown in Fig 4. No other similar peak was found in the
347 entire record which may indicate a specific event to lead to this sharp increased,
348 which provide useful information to track the BC emissions. In this study, we conduct
349 several model studies to investigate this special event.

350
351 As shown in Figure 4, there was a high BC deposition flux (900 ng cm⁻²) in 1992,
352 compared to 100-300 ng cm⁻² in other years. In order to investigate this special event,
353 we focus our model study on a short period (from 1986 to 1994). One potential reason
354 to cause this sharp increase of BC was that during 1991, when Iraqi troops withdrew
355 from Kuwait at the end of the first Gulf War, they setted a huge fire over 700 oil wells.
356 The fires were started in January and February 1991, and the last well was capped on
357 November 6, 1991. The resulting fires produced a large plume of smoke and particles
358 that had significant effects on the Persian Gulf area and the potential for global effects
359 (as shown in Fig. 5).

360
361
362
363
364
365
366
367
368
369
370
371
372
373
374
375
376
377
378
379
380
381
382
383
384
385
386
387
388
389
390
391
392
393

In order to estimate intensive of the BC emission from the fires, (Hobbs and Radke (1992), conducted two aircraft studies during the period 16 May through 12 June 1991 to evaluate the effects of the smoke. The estimated emission rate of elemental carbon of the Kuwait fires is ~3400 metric tons per day which is 13 times the BC emissions from all U.S. combustion sources in total.

带格式的: 字体: 小四

带格式的: 字体: 小四

In order to study the effect of the huge Kuwait fires on the BC ice core deposition, the MOZART-4 model was applied to simulate the atmospheric BC concentrations and deposition fluxes variation from 1986 to 1994. Several model sensitive studies were conducted. First, the atmospheric BC concentration was calculated by the anthropogenic BC emission with the default emissions (POET) as described before. Second, in order to simulate the large increase in the BC emissions caused by the Kuwait fires in Persian Gulf (Region 3 in Fig. 1), according to the measured values of Hobbs and Radke (1992), the BC emissions were significantly enhanced by 50 times from January to November, 1991 to represent Kuwait fires. Figure 4 shows the horizontal distribution of the calculated BC plume from the Kuwait fires, with the enhanced BC emission.

带格式的: 字体: 小四, 突出显示

带格式的: 字体: 小四

带格式的: 字体: 小四

带格式的: 字体: 小四

The calculated result suggests that there was a significant increase of BC concentrations nearby the Kuwait fires (see Fig. 6). The BC concentrations reached to 10-20 $\mu\text{g m}^{-3}$ at the surface (see Fig. 6A) and more than 0.7 $\mu\text{g m}^{-3}$ at 5 km above the surface (see Fig. 6B). As shown in Figs. 5 and 6, the winds nearby the fire region were toward to northern and northwestern directions. Because the lifetime of black carbon aerosols is sufficiently long (about a week) (Ramanathan et al., 2001; Bauer et al., 2013), the high BC concentrations were transported westerly toward the Muztagh Ata Mountain.

带格式的: 字体: 小四

带格式的: 字体: 小四

The evaluation of the modeled BC deposition at the Muztagh Ata Mountain was conducted by comparison between the calculation and measurement (see Fig. 4). Figure 4 shows the calculated temporal variation of BC concentrations and deposition, which were compared with the measured variations. The result shows that the calculated temporal variability of BC deposition was generally consistent with the

394 measured variability. For example, the both high peaks of calculated and measured
395 BC deposition occurred in 1992. The calculated atmospheric concentrations of BC,
396 however, had a peak value in 1991. This was due to the fact that the deposition of BC
397 in ice core was an accumulated value, while the atmospheric BC concentration was an
398 in-situ value. Despite of the consistence of temporal variations between measured and
399 calculated deposition of BC, there was a consistent underestimate of calculated BC
400 deposition compared to the measured value. Because there were uncertainties in
401 estimates BC emission and the deposition, these uncertainties could result in the
402 discrepancy between the calculation and measurement. For example, according to the
403 assimilation meteorological data by Chinese Meteorological Admiration, the annual
404 precipitation in 1992 was about twice higher than in 1991 nearby Muztagh Ata
405 Mountain, suggesting that scavenging efficiency may likely underestimated, causing
406 the calculated uncertainty in the estimate of the BC deposition.

407

408 3.3 Effect of regional BC emissions at the Muztagh Ata Mountain

409

410 To further understand the influence of transportation and deposition on the annual
411 variation of BC at the Muztagh Ata Mountain (as a receptor region), sensitivity
412 experiments using the MOZART-4 model were conducted. In the sensitive study, the
413 effect of different BC emission regions on the BC concentrations at the measurement
414 site was individually calculated. Four primary regions were defined with latitude and
415 longitude, as shown in Table 1 and Fig. 1, including (R1) Central Asia, (R2) Europe,
416 (R3) Persian Gulf, and (R4) South Asia. Central Asia, Europe and South Asia
417 previously have been reported as significant BC emission sources of Muztagh Ata
418 Mountain (Liu et al., 2008; Xu et al., 2009a; Wang et al., 2015b). Europe is one of
419 the biggest emission sources of the world located in the upwind region of receptor
420 site although it is far away. Central Asia and South Asia are surrounding emission
421 sources of the receptor site. Persian Gulf could be a potentially emission source
422 which could be overlooked before. In each sensitive study, only the individual BC
423 emission was included, and the BC emissions in other regions were excluded. As a
424 result, the fractional contributions by the individual emission regions to BC
425 concentrations in the receptor region (the Muztagh Ata Mountain) were calculated.
426 Table 1 shows the calculated results.

427

带格式的: 字体: 小四, 突出显示

带格式的: 字体: 小四

带格式的: 字体: 小四, 突出显示

带格式的: 字体: 小四

带格式的: 字体: 小四, 突出显示

带格式的: 字体: 小四

带格式的: 字体: 小四

带格式的: 字体: 小四, 突出显示

带格式的: 字体: 小四

带格式的: 字体: 小四, 突出显示

带格式的: 字体: 小四

428 In order to clearly show the transport pathways from the different regions to the
429 measurement site and the Tibetan Plateau, the calculated horizontal distributions of
430 BC concentrations from each region during 3 different periods (summer monsoon,
431 non-monsoon, and annual mean) were shown in Fig. 7.

432
433 The results from Table 1 and Fig. 7 suggests that during the “normal period” (non
434 Kuwait Fires), the BC emissions from Central Asia and South Asia had the largest
435 contributions to the BC concentrations at measurement site, contributing annual mean
436 of 27% and 25%, respectively. It is interesting to note that there were strong seasonal
437 variations regarding the effects. During the monsoon period, the largest effect was due
438 to the Central Asia source (44%), while during non-monsoon period, the largest effect
439 was due to the South Asia source (34%).

440
441 As shown in Fig. 7, during the monsoon period, the airflow from the oceans (Persian
442 Gulf and Bengal Bay) moves northward and coupled with the strong precipitation.
443 As a result, the BC particles from south Asian source were washout during the
444 transport pathway, leading to lower BC concentrations at the measurement site. In
445 contrast, during the non-monsoon period, the prevailing winds were western winds,
446 which BC emission in the northern India was transported to the measurement site
447 measurement site, leading to higher BC concentrations. The contributions from
448 Persian Gulf emissions were generally low to the BC concentrations. However during
449 Kuwait fires period, this region had significant contribution to the Muztagh Ata area
450 as well as the Tibetan Plateau.

451 452 **3.4 Radiative forcing induced by BC in Muztagh Ata glacier**

453
454 The deposition of BC on the snow reduces the surface albedo, causing a positive
455 radiative forcing and increases in ice and snow melt. Previous studies show that BC
456 particles produce significant reduction in the snow albedo, with the solar visible
457 wavelengths (Warren and Wiscombe, 1980). In this study, the effect of BC deposition
458 on the snow albedo and radiative forcing during 1986 to 1994 in Muztagh Ata glacier
459 was estimated. The SINICAR model (Snow, Ice, and Aerosol Radiation; available at
460 <http://snow.engin.umich.edu>) was used to estimate the effect of BC particles on snow
461 albedo in different solar wavelengths (Flanner and Zender, 2005; Flanner et al., 2007).

带格式的：字体：小四

带格式的：字体：小四

带格式的：默认段落字体，字体：
(默认)+西文正文，小四，字体颜色：
自动设置

带格式的：字体：小四，无下划线

带格式的：字体：小四，无下划线

带格式的：字体：小四，无下划线

带格式的：字体：小四

462

463 To estimate the effect of the BC deposition on surface albedo, in addition to the BC
464 concentrations, there are several environmental factors such as snow grain size, solar
465 zenith angle, and snow depth were needed to be estimated (Warren and Wiscombe,
466 1980). The setup of input parameters required for running the SNICAR model is
467 briefly described as below. As we focus on the calculation of radiative forcing caused
468 by BC particles, other impurity contents, such as dust and volcanic ash, were set to be
469 zero. A mass absorption cross section (MAC) of $7.5 \text{ m}^2 \text{ g}^{-1}$ at 550 nm for uncoated BC
470 particles (Bond and Bergstrom, 2006) was assumed to be same as the default value,
471 and the MAC scaling factor in the online SNICAR model as one of input parameters
472 was set to be 1.0. The effective radius of $100 \text{ }\mu\text{m}$ with a density of 60 kg m^{-3} was used
473 for new snow, and the effective radius of $400 \text{ }\mu\text{m}$ with a density of 400 kg m^{-3} was
474 adopted for the albedo estimation according to the previous studies and measurements
475 in other studies in Tibetan Plateau (Wiscombe and Warren, 1980; Wu et al., 2006).
476 The extractive snow height from MERRA (the Modern-Era Retrospective-analysis for
477 Research and Applications) reanalysis products was used for snowpack thickness. The
478 forcing dataset used in this study was developed by Data Assimilation and Modeling
479 Center for Tibetan Multi-spheres, Institute of Tibetan Plateau Research, Chinese
480 Academy of Sciences (Chen et al., 2011). The recovered BC concentrations of ice
481 core were used as the input parameter of uncoated black carbon concentration. The
482 averaged short-wave flux and solar zenith angle of each month were obtained from
483 China Meteorological Forcing Dataset provided by Data Assimilation and Modeling
484 Center for Tibetan Multi-spheres, Institute of Tibetan Plateau Research, Chinese
485 Academy of Sciences.

带格式的: 字体: 小四, 无下划线

带格式的: 字体: 小四, 无下划线

带格式的: 字体: 小四, 无下划线

带格式的: 字体: 小四, 无下划线

带格式的: 字体: 小四, 无下划线

带格式的: 字体: 小四, 无下划线

带格式的: 字体: 小四, 无下划线

带格式的: 字体: 小四, 无下划线

带格式的: 字体: 小四, 无下划线

带格式的: 字体: 小四

486

487 The measured average BC concentration in ice core during 1986-1994 was 15.2 ng g^{-1} ,
488 with a peak value of 39.2 ng g^{-1} . The calculated snow albedo reduction by using the
489 SNICAR model ranged from 0.11% to 1.36% by assuming that the snow layer was
490 totally covered by fresh snow (lower limit). However, if it was aged layer, the
491 estimated snow albedo reduction increased, ranging from 0.47% to 2.97% (upper
492 limit). The actual value should be lied between the two ranges. This result is
493 consistent with the previous studies. For example, (Yasunari et al., 2010) reported that
494 the reduction of snow albedo ranged from 2.0% to 5.2%, with the BC concentration of
495 26.0-68.2 ng/g, based on atmospheric BC measurements at NCO-P over the southern

带格式的: 字体: 小四, 无下划线

带格式的: 字体: 小四, 无下划线

带格式的: 字体: 小四, 无下划线

496 slopes of western Himalayas.

带格式的: 字体: 小四

497

498 The reduction of snow albedo enhanced the absorption of solar energy and accelerated
499 snow and ice melt (Conway et al., 1996). Several studies suggested that that BC
500 containments on snow were very effective to reduce the surface albedo (Warren and
501 Wiscombe, 1980; Petr Chylek and Srivastava, 1983; Gardner and Sharp, 2010). In this
502 study, the effects of BC containments on snow albedo and snow water equivalent
503 (SWE) reduction were estimated.

带格式的: 字体: 小四, 无下划线

带格式的: 字体: 小四, 无下划线

带格式的: 字体: 小四, 无下划线

带格式的: 字体: 小四, 无下划线

带格式的: 字体: 小四, 无下划线

带格式的: 字体: 小四

504

505 Figure 8 shows the calculated the effects of BC containments on annual mean
506 radiative forcing increase (RFI) ($W m^{-2}$) and snow water equivalent (SWE) reduction
507 ($mm yr^{-1}$; millimeter per year), under fresh snow assumption and aged snow
508 assumption. The results show that under the fresh snow assumption (lower limit), the
509 increases of RFI ranged from $0.2 W m^{-2}$ to $2.5 W m^{-2}$, while under the aged snow
510 assumption (upper limit), the increases of RFI ranged from $0.9 W m^{-2}$ to $5.7 W m^{-2}$.
511 This estimate is consistent with the previous studies (Flanner et al., 2009). During the
512 Kuwait fires period, the RFI values increased about 2-5 times higher, which led to a
513 significant increase for the snow melting during the period.

带格式的: 字体: 小四, 无下划线

带格式的: 字体: 小四, 无下划线

带格式的: 字体: 小四, 无下划线

带格式的: 字体: 小四

514

515 ~~The runoff of the melted snow due to the increase of snow surface albedo was~~
516 ~~estimated in this study.~~ The potential influence for BC deposition on ~~galciersglaciers~~
517 from forest fires was highlighted that was coincident with an increase discharge in the
518 downriver in previous study (Kaspari et al., 2015). The runoff of the melted snow due
519 to the increase of snow surface albedo was estimated in this study. A first-order
520 estimation was based on the additional energy contribution to the snowpack due to BC
521 deposition. First the melting point of snow was estimated. Second, the extra snow
522 melt from light absorbing black carbon was estimated by dividing hourly
523 instantaneous radiative forcing, with the enthalpy of fusion of water at $0^{\circ}C$ of $0.334 \times$
524 $10^6 J kg^{-1}$ (Painter et al., 2013; Kaspari et al., 2015). The estimation represented the
525 snow melt in $kg m^{-2}$ across the hour during acquisition translates, or melt in mm of
526 snow water equivalent (SWE). The melted snow due to the BC water was calculated
527 (shown in Fig. 8). The result shows that the estimated averaged SWE reductions were
528 111 mm and 270 mm, for fresh and aged snow respectively. During the Kuwait fires

带格式的: 字体: 小四, 无下划线

带格式的: 字体: 小四, 无下划线, 突出显示

带格式的: 字体: 小四, 无下划线

带格式的: 字体: 小四, 无下划线, 突出显示

带格式的: 字体: 小四, 无下划线

带格式的: 字体: 小四, 无下划线, 突出显示

带格式的: 字体: 小四, 无下划线

带格式的: 字体: 小四, 无下划线, 突出显示

带格式的: 字体: 小四, 无下划线

带格式的: 字体: 小四, 无下划线

带格式的: 字体: 小四, 无下划线

带格式的: 字体: 小四, 无下划线, (国际) Times New Roman

带格式的: 字体: 小四, 无下划线

带格式的: 字体: 小四, 无下划线

带格式的: 字体: 小四, 无下划线

529 period, the estimated SWE significantly increased, reaching to 600 mm for aged snow
530 condition, and 300 mm for fresh snow condition. The increase was about 3 times than
531 pre- and post- Kuwait fires, suggesting that this special event had a significant impact
532 on snow melting for the Tibetan glaciers and the water resources in the region.
533 However, this estimate of runoff is speculative since there are a number of influential
534 factors. (Schmale et al., (2017), found that combination effect of meteorological
535 parameters and snow albedo could be 3 times larger than model results. The Tibetan
536 Plateau is recognized as “Water Tower of Asia” with largely contribution to annual
537 river discharge of Yangtze River, Indus and Brahmaputra etc. The snowmelt runoff
538 will impact on regional climate system including the timing of runoff- the frequency
539 and intensity of floods and rainfall patterns because of since its tightening interactive
540 with the hydrologic cycle (Jain et al., 2010). Wu and Qian (2003) reported that
541 Tibetan winter snow cover is anormalyabnormally-is linked to rainfall over south,
542 southeast and east Asia by observation data analysis.

543 **4 Conclusions**

544 Black carbon (BC) particles change the radiative balance of the atmosphere by
545 absorbing and scattering solar radiation. As a result, BC deposition on the surface of
546 snow and ice changes the albedo of solar radiation. Albedo change is the key
547 parameter to affect the melting of glacier in Tibetan Plateau. In order to study this
548 effect, two sets of measurements were used to study the variability of BC deposition
549 at Muztagh Ata Mountain, Northern Tibetan Plateau. The measured data included the
550 air samplings of BC particles during 2004-2006 and the ice core drillings of BC
551 deposition during 1986-1994. To identify the effect of BC emissions on the BC
552 deposition in this region, a global chemical transportation model (MOZART-4) was
553 used to analyze the BC transport from the source regions. A radiative transfer model
554 (SNICAR) was used to study the effect of BC deposition on snow albedo.

555
556 The results show some important highlights to reveal the temporal variability of BC
557 deposition and the effect of long-rang transport on the BC pollution in the Northern
558 Tibetan Plateau, which are summarized as the follows;

559 (1) During 1991-1992, there was a strong spike of the BC deposition at Muztagh
560 Ata, suggesting that there was unusual emission in the upward region. This

带格式的: 字体: 小四, 无下划线, 突出显示

带格式的: 字体: 小四, 无下划线

带格式的: 字体: 小四, 无下划线, 突出显示

带格式的: 字体: 小四, 无下划线

带格式的: 字体: 小四, 无下划线, 突出显示

带格式的: 字体: 小四, 无下划线

带格式的: 字体: 小四, 无下划线, 突出显示

带格式的: 字体: 小四, 无下划线

带格式的: 字体: 小四, 无下划线, 突出显示

带格式的: 字体: 小四, 无下划线

带格式的: 字体: 小四, 无下划线, 突出显示

带格式的: 字体: 小四, 无下划线

带格式的: 字体: 小四, 无下划线, 突出显示

带格式的: 字体: 小四, 无下划线

带格式的: 字体: 小四, 无下划线

带格式的: 字体: 小四, 无下划线

带格式的: 字体: 小四, 无下划线, 突出显示

带格式的: 字体: 小四, 无下划线, 突出显示

带格式的: 字体: 小四, 无下划线, 突出显示

带格式的: 字体: 小四, 无下划线

带格式的: 字体: 小四

带格式的: 字体: 小四, 无下划线

带格式的: 字体: 小四

带格式的: 字体: 小四, 无下划线

带格式的: 字体: 小四

带格式的: 字体: 小四, 无下划线

带格式的: 字体: 小四

带格式的: 字体: 小四, 无下划线

带格式的: 字体: 小四

带格式的: 字体: 小四

带格式的: 字体: 小四, 无下划线

561 high peak of BC deposition was investigated by using the global chemical
562 transportation model (MOZART-4). The analysis indicated that the emissions
563 from large Kuwait fires at the end of the first Gulf War in 1991 caused the
564 high peak of the BC concentrations and the BC deposition. As a result, the BC
565 deposition in 1991 and 1992 at the Muztagh Ata Mountain was 3-4 times
566 higher than other periods.

带格式的: 字体: 小四

567 (2) The effect of Kuwait fires on the BC deposition at the Muztagh Ata Mountain
568 suggested that the upward BC emissions had important impacts on this remote
569 site located in Northern Tibetan Plateau. In order to quantitatively estimate the
570 effect of surrounding emissions on the BC concentrations in the northern
571 Tibetan Plateau, a sensitive study with 4 individual BC emission regions
572 (Central Asia, Europe, Persian Gulf, and South Asia) was conducted by using
573 the MOZART-4 model. The result suggests that during the “normal period”
574 (non Kuwait Fires), the largest effect was due to the Central Asia source (44%)
575 during Indian monsoon period. During non-monsoon period, the largest effect
576 was due to the South Asia source (34%).

带格式的: 字体: 小四, 无下划线

577 (3) The increase of radiative forcing increase (RFI) due to the deposition of BC on
578 snow was estimated by using the radiative transfer model (SNICAR). The
579 results show that under the fresh snow assumption, the estimated RFI ranged
580 from 0.2 W m^{-2} to 2.5 W m^{-2} , while under the aged snow assumption, the
581 estimated RFI ranged from 0.9 W m^{-2} to 5.7 W m^{-2} . During the Kuwait fires
582 period, the RFI values increased about 2-5 times higher than the “normal
583 period”, suggesting a significant increase for the snow melting in Northern
584 Tibetan Plateau due to this fire event.

带格式的: 字体: 小四

带格式的: 字体: 小四, 无下划线

585
586 This result suggests that the variability of BC deposition at the Muztagh Ata
587 Mountain provides useful information to study the effect of the upward BC emissions
588 on environmental and climate issues in the Northern Tibetan Plateau. The radiative
589 effect of BC deposition on the snow melting provides important information regarding
590 the water resources in the region.

带格式的: 字体: 小四

带格式的: 字体: 小四, 无下划线

带格式的: 字体: 小四

带格式的: 字体: 小四, 无下划线

带格式的: 字体: 小四

带格式的: 字体: 小四, 无下划线

带格式的: 字体: 小四

带格式的: 字体: 小四, 无下划线,
字体颜色: 自动设置

592 **Acknowledgement**

593 This work was supported by the National Natural Science Foundation of China
594 (NSFC) under Grant Nos. 41430424 and 41730108 and 41230641. The Authors

带格式的: 字体: 小四, 无下划线,
字体颜色: 自动设置, 突出显示

带格式的: 字体: 小四, 无下划线,
字体颜色: 自动设置

595 | thanks the supports of Center for Excellence in Urban Atmospheric Environment,
596 | Institute of Urban Environment, Chinese Academy of Sciences. The National Center
597 | for Atmospheric Research is sponsored by the National Science Foundation.
598 |
599 |

带格式的: 字体: 小四

带格式的: 字体: Times New Roman, 小四

600

References

601 An, Z. S., Kutzbach, J. E., Prell, W. L., and Porter, S. C.: Evolution of Asian
602 monsoons and phased uplift of the Himalaya-Tibetan plateau since Late Miocene
603 times, *Nature*, 411, 62–66, doi:10.1038/35075035, 2001.

带格式的: 字体: Times New Roman, 小四, 无下划线, 字体颜色: 自动设置

604 Bauer, S. E., Bausch, A., Nazarenko, L., Tsigaridis, K., Xu, B., Edwards, R., Bisiaux,
605 M., and McConnell, J.: Historical and future black carbon deposition on the three
606 ice caps: Ice core measurements and model simulations from 1850 to 2100, *J.*
607 *Geophys. Res. Atmos.*, 118, 7948–7961, doi:10.1002/jgrd.50612, 2013.

带格式的: 字体: Times New Roman, 小四

带格式的: 字体: Times New Roman, 小四, 无下划线, 字体颜色: 自动设置

608 Bisiaux, M. M., Edwards, R., McConnell, J. R., Curran, M. A. J., van Ommen, T. D.,
609 Smith, A. M., Neumann, T. A., Pasteris, D. R., Penner, J. E., and Taylor, K.:
610 Changes in black carbon deposition to Antarctica from two high-resolution ice
611 core records, 1850–2000 AD, *Atmos. Chem. Phys.*, 12, 4107–4115,
612 doi:10.5194/acp-12-4107-2012, 2012.

带格式的: 字体: Times New Roman, 小四

带格式的: 字体: Times New Roman, 小四, 无下划线, 字体颜色: 自动设置

613 Bond, T. C. and Bergstrom, R. W.: Light Absorption by Carbonaceous Particles: An
614 Investigative Review, *Aerosol Sci. Tech.*, 40, 27–67,
615 doi:10.1080/02786820500421521, 2006.

带格式的: 字体: Times New Roman, 小四

带格式的: 字体: Times New Roman, 小四, 无下划线, 字体颜色: 自动设置

616 Bond, T. C., Streets, D. G., Yarber, K. F., Nelson, S. M., Woo, J.-H., and Klimont, Z.:
617 A technology-based global inventory of black and organic carbon emissions from
618 combustion, *J. Geophys. Res.*, 109, 1042, doi:10.1029/2003JD003697, 2004.

带格式的: 字体: Times New Roman, 小四

带格式的: 字体: Times New Roman, 小四, 无下划线, 字体颜色: 自动设置

619 Brasseur, G. P., Hauglustaine, D. A., Walters, S., Rasch, P. J., Müller, J.-F., Granier, C.,
620 and Tie, X. X.: MOZART, a global chemical transport model for ozone and related
621 chemical tracers: 1. Model description, *J. Geophys. Res.*, 103, 28265–28289,
622 doi:10.1029/98JD02397, 1998.

带格式的: 字体: Times New Roman, 小四

带格式的: 字体: Times New Roman, 小四, 无下划线, 字体颜色: 自动设置

623 Cao, J. J., Lee, S. C., Ho, K. F., Zhang, X. Y., Zou, S. C., Fung, K., Chow, J. C., and
624 Watson, J. G.: Characteristics of carbonaceous aerosol in Pearl River Delta Region,
625 China during 2001 winter period, *Atmos. Environ.*, 37, 1451–1460,
626 doi:10.1016/S1352-2310(02)01002-6, 2003.

带格式的: 字体: Times New Roman, 小四

带格式的: 字体: Times New Roman, 小四, 无下划线, 字体颜色: 自动设置

627 Cao, J. J., Xu, B. Q., He, J. Q., Liu, X. Q., Han, Y. M., Wang, G. H., and Zhu, C. S.:
628 Concentrations, seasonal variations, and transport of carbonaceous aerosols at a
629 remote Mountainous region in western China, *Atmos. Environ.*, 43, 4444–4452,
630 2009.

带格式的: 字体: Times New Roman, 小四

带格式的: 字体: Times New Roman, 小四, 无下划线, 字体颜色: 自动设置

631 Chang, L. Y., Xu, J. M., Tie, X. X., and Wu, J. B.: Impact of the 2015 El Nino event
632 on winter air quality in China, *Sci. Rep.*, 6, 34275, doi:10.1038/srep34275, 2016.

带格式的: 字体: Times New Roman, 小四

带格式的: 字体: Times New Roman, 小四, 无下划线, 字体颜色: 自动设置

633 Chen, Y., Yang, K., He, J., Qin, J., Shi, J., Du, J., and He, Q.: Improving land surface
634 temperature modeling for dry land of China, *J. Geophys. Res.*, 116, 251,
635 doi:10.1029/2011JD015921, 2011.

带格式的: 字体: Times New Roman, 小四

带格式的: 字体: Times New Roman, 小四, 无下划线, 字体颜色: 自动设置

636 Chow, J. C., Watson, J. G., Chen, L. W. A., Arnott, W. P., Moosmüller, H., and Fung,
637 K.: Equivalence of elemental carbon by thermal/optical reflectance and
638 transmittance with different temperature protocols, *Environ. Sci. Technol.*, 38,
639 4414–4422, 2004.

带格式的: 字体: Times New Roman, 小四

带格式的: 字体: Times New Roman, 小四, 无下划线, 字体颜色: 自动设置

640 Chow, J. C., Watson, J. G., Pritchett, L. C., Pierson, W. R., Frazier, C. A., and Purcell,
641 R. G.: The dri thermal/optical reflectance carbon analysis system: Description,

带格式的: 字体: Times New Roman, 小四

带格式的: 字体: Times New Roman, 小四, 无下划线, 字体颜色: 自动设置

642	evaluation and applications in U.S. Air quality studies, <i>Atmos. Environ. Part A. General Topics.</i> , 27, 1185–1201, doi:10.1016/0960-1686(93)90245-T, 1993.	带格式的: 字体: Times New Roman, 小四
643		
644	Conway, H., Gades, A., and Raymond, C. F.: Albedo of dirty snow during conditions	带格式的: 字体: Times New Roman, 小四, 无下划线, 字体颜色: 自动设置
645	of melt, <i>Water Resour. Res.</i> , 32, 1713–1718, doi:10.1029/96WR00712, 1996.	
646	Cooke, W. F. and Wilson, J. J. N.: A global black carbon aerosol model, <i>J. Geophys. Res.</i> , 101, 19395–19409, doi:10.1029/96JD00671, 1996.	带格式的: 字体: Times New Roman, 小四
647		
648	Emmons, L. K., Walters, S., Hess, P. G., Lamarque, J.-F., Pfister, G. G., Fillmore, D.,	带格式的: 字体: Times New Roman, 小四, 无下划线, 字体颜色: 自动设置
649	Granier, C., Guenther, A., Kinnison, D., Laepple, T., Orlando, J., Tie, X., Tyndall,	带格式的: 字体: Times New Roman, 小四
650	G., Wiedinmyer, C., Baughcum, S. L., and Kloster, S.: Description and evaluation	带格式的: 字体: Times New Roman, 小四, 无下划线, 字体颜色: 自动设置
651	of the Model for Ozone and Related chemical Tracers, version 4 (MOZART-4),	带格式的: 字体: Times New Roman, 小四, 无下划线, 字体颜色: 自动设置
652	<i>Geosci. Model Dev.</i> , 3, 43–67, doi:10.5194/gmd-3-43-2010, 2010.	
653	Fang, Y., Chen, Y. J., Tian, C. G., Lin, T., Hu, L. M., Huang, G. P., Tang, J. H., Li, J.,	带格式的: 字体: Times New Roman, 小四
654	and Zhang, G.: Flux and budget of BC in the continental shelf seas adjacent to	带格式的: 字体: Times New Roman, 小四, 无下划线, 字体颜色: 自动设置
655	Chinese high BC emission source regions, <i>Global Biogeochem. Cycles</i> , 29,	
656	957–972, doi:10.1002/2014GB004985, 2015.	带格式的: 字体: Times New Roman, 小四
657	Flanner, M. G. and Zender, C. S.: Snowpack radiative heating: Influence on Tibetan	带格式的: 字体: Times New Roman, 小四
658	Plateau climate, <i>Geophys. Res. Lett.</i> , 32, 10,219, doi:10.1029/2004GL022076,	带格式的: 字体: Times New Roman, 小四, 无下划线, 字体颜色: 自动设置
659	2005.	
660	Flanner, M. G., Zender, C. S., Hess, P. G., Mahowald, N. M., Painter, T. H.,	带格式的: 字体: Times New Roman, 小四
661	Ramanathan, V., and Rasch, P. J.: Springtime warming and reduced snow cover	带格式的: 字体: Times New Roman, 小四, 无下划线, 字体颜色: 自动设置
662	from carbonaceous particles, <i>Atmos. Chem. Phys.</i> , 9, 2481–2497,	
663	doi:10.5194/acp-9-2481-2009, 2009.	带格式的: 字体: Times New Roman, 小四
664	Flanner, M. G., Zender, C. S., Randerson, J. T., and Rasch, P. J.: Present-day climate	带格式的: 字体: Times New Roman, 小四
665	forcing and response from black carbon in snow, <i>J. Geophys. Res.</i> , 112, 3131,	带格式的: 字体: Times New Roman, 小四, 无下划线, 字体颜色: 自动设置
666	doi:10.1029/2006JD008003, 2007.	
667	Gardner, A. S. and Sharp, M. J.: A review of snow and ice albedo and the	带格式的: 字体: Times New Roman, 小四
668	development of a new physically based broadband albedo parameterization, <i>J.</i>	带格式的: 字体: Times New Roman, 小四, 无下划线, 字体颜色: 自动设置
669	<i>Geophys. Res.</i> , 115, D13203, doi:10.1029/2009JF001444, 2010.	
670	Hack, J. J.: Parameterization of moist convection in the National Center for	带格式的: 字体: Times New Roman, 小四, 无下划线, 字体颜色: 自动设置
671	Atmospheric Research community climate model (CCM2), <i>J. Geophys. Res.</i> , 99,	
672	5551, doi:10.1029/93JD03478, 1994.	带格式的: 字体: Times New Roman, 小四
673	Hagen, D. E., Trueblood, M. B., and Whitefield, P. D.: A Field Sampling of Jet	带格式的: 字体: Times New Roman, 小四, 无下划线, 字体颜色: 自动设置
674	Exhaust Aerosols, <i>Particulate Sc. & Tech.</i> , 10, 53–63,	
675	doi:10.1080/02726359208906598, 1992.	带格式的: 字体: Times New Roman, 小四
676	Hansen, J. and Nazarenko, L.: Soot climate forcing via snow and ice albedos, <i>P. Natl.</i>	带格式的
677	<i>Acad. Sci. USA</i> , 101, 423–428, 2004.	带格式的: 字体: Times New Roman, 小四
678	Hobbs, P. V. and Radke, L. F.: Airborne studies of the smoke from the kuwait oil fires,	带格式的
679	<i>Science</i> , 256, 987–991, doi:10.1126/science.256.5059.987, 1992.	带格式的
680	Holben, B. N., Eck, T. F., Slutsker, I., Tanr é D., Buis, J. P., Setzer, A., Vermote, E.,	带格式的: 字体: Times New Roman, 小四
681	Reagan, J. A., Kaufman, Y. J., Nakajima, T., Lavenu, F., Jankowiak, I., and	带格式的
682	Smirnov, A.: AERONET—A Federated Instrument Network and Data Archive for	带格式的: 字体: Times New Roman, 小四
683	Aerosol Characterization, <i>Remote Sens. Environ.</i> , 66, 1–16,	带格式的
684	doi:10.1016/S0034-4257(98)00031-5, 1998.	带格式的
685	Holtslag, A. A. M. and Boville, B. A.: Local Versus Nonlocal Boundary-Layer	带格式的: 字体: Times New Roman, 小四
		带格式的

686 Diffusion in a Global Climate Model, *J. Climate*, 6, 1825–1842,
687 doi:10.1175/1520-0442(1993)006<1825:LVNBLD>2.0.CO;2, 1993.

688 Jain, S. K., Goswami, A., and Saraf, A. K.: Assessment of Snowmelt Runoff Using
689 Remote Sensing and Effect of Climate Change on Runoff, *Water Resour Manage*,
690 24, 1763–1777, doi:10.1007/s11269-009-9523-1, 2010.

691 Jurado, E., Dachs, J., Duarte, C. M., and Simó R.: Atmospheric deposition of organic
692 and black carbon to the global oceans, *Atmos. Environ.*, 42, 7931–7939,
693 doi:10.1016/j.atmosenv.2008.07.029, 2008.

694 Jurado, E., Jaward, F., Lohmann, R., Jones, K. C., Simó R., and Dachs, J.: Wet
695 Deposition of Persistent Organic Pollutants to the Global Oceans, *Environ. Sci.*
696 *Technol.*, 39, 2426–2435, doi:10.1021/es048599g, 2005.

697 Kaspari, S., McKenzie Skiles, S., Delaney, I., Dixon, D., and Painter, T. H.:
698 Accelerated glacier melt on Snow Dome, Mount Olympus, Washington, USA, due
699 to deposition of black carbon and mineral dust from wildfire, *J. Geophys. Res.*
700 *Atmos.*, 120, 2793–2807, doi:10.1002/2014JD022676, 2015.

701 Kaspari, S. D., Schwikowski, M., Gysel, M., Flanner, M. G., Kang, S., Hou, S., and
702 Mayewski, P. A.: Recent increase in black carbon concentrations from a Mt.
703 Everest ice core spanning 1860–2000 AD, *Geophys. Res. Lett.*, 38, n/a-n/a,
704 doi:10.1029/2010GL046096, 2011.

705 Kinnison, D. E., Brasseur, G. P., Walters, S., Garcia, R. R., Marsh, D. R., Sassi, F.,
706 Harvey, V. L., Randall, C. E., Emmons, L., Lamarque, J. F., Hess, P., Orlando, J. J.,
707 Tie, X. X., Randel, W., Pan, L. L., Gettelman, A., Granier, C., Diehl, T., Niemeier,
708 U., and Simmons, A. J.: Sensitivity of chemical tracers to meteorological
709 parameters in the MOZART-3 chemical transport model, *J. Geophys. Res.*, 112,
710 32295, doi:10.1029/2006JD007879, 2007.

711 Lavanchy, V.M.H., Gäggeler, H. W., Schotterer, U., Schwikowski, M., and
712 Baltensperger, U.: Historical record of carbonaceous particle concentrations from
713 a European high-alpine glacier (Colle Gnifetti, Switzerland), *J. Aerosol Sci.*, 30,
714 S611-S612, doi:10.1016/S0021-8502(99)80316-4, 1999.

715 Li, C. L., Yan, F. P., Kang, S. C., Chen, P. F., Han, X. W., Hu, Z. F., Zhang, G. S.,
716 Hong, Y., Gao, S. P., Qu, B., Zhu, Z. J., Li, J. W., Chen, B., and Sillanpää M.:
717 Re-evaluating black carbon in the Himalayas and the Tibetan Plateau:
718 Concentrations and deposition, *Atmos. Chem. Phys.*, 17, 11899–11912,
719 doi:10.5194/acp-17-11899-2017, 2017.

720 Lin, S.-J. and Rood, R. B.: Multidimensional Flux-Form Semi-Lagrangian Transport
721 Schemes, *Mon. Wea. Rev.*, 124, 2046–2070,
722 doi:10.1175/1520-0493(1996)124<2046:MFFSLT>2.0.CO;2, 1996.

723 Liousse, C., Cachier, H., and Jennings, S. G.: Optical and thermal measurements of
724 black carbon aerosol content in different environments: Variation of the specific
725 attenuation cross-section, sigma (σ), *Atmospheric Environment. Part A. General*
726 *Topics*, 27, 1203–1211, doi:10.1016/0960-1686(93)90246-U, 1993.

727 Liu, X. Q., Xu, B. Q., Yao, T. D., Wang, N. L., and Wu, G. J.: Carbonaceous particles
728 in Muztagh Ata ice core, West Kunlun Mountains, China, *Sci. Bull.*, 53,
729 3379–3386, doi:10.1007/s11434-008-0294-5, 2008.

带格式的: 字体: Times New Roman, 小四

带格式的: 字体: Times New Roman, 小四, 无下划线, 字体颜色: 自动设置

带格式的: 字体: Times New Roman, 小四

带格式的: 字体: Times New Roman, 小四, 无下划线, 字体颜色: 自动设置

带格式的: 字体: Times New Roman, 小四

带格式的: 字体: Times New Roman, 小四, 无下划线, 字体颜色: 自动设置

带格式的: 字体: Times New Roman, 小四

带格式的: 字体: Times New Roman, 小四, 无下划线, 字体颜色: 自动设置

带格式的: 字体: Times New Roman, 小四

带格式的: 字体: Times New Roman, 小四, 无下划线, 字体颜色: 自动设置

带格式的: 字体: Times New Roman, 小四

带格式的: 字体: Times New Roman, 小四, 无下划线, 字体颜色: 自动设置

带格式的: 字体: Times New Roman, 小四

带格式的: 字体: Times New Roman, 小四, 无下划线, 字体颜色: 自动设置

带格式的: 字体: Times New Roman, 小四

带格式的: 字体: Times New Roman, 小四, 无下划线, 字体颜色: 自动设置

带格式的: 字体: Times New Roman, 小四

带格式的: 字体: Times New Roman, 小四, 无下划线, 字体颜色: 自动设置

带格式的: 字体: Times New Roman, 小四

带格式的: 字体: Times New Roman, 小四, 无下划线, 字体颜色: 自动设置

带格式的: 字体: Times New Roman, 小四

730 Mackay, D., Paterson, S., and Schroeder, W. H.: Model describing the rates of transfer
731 processes of organic chemicals between atmosphere and water, Environ. Sci.
732 Technol., 20, 810–816, doi:10.1021/es00150a009, 1986.

733 McConnell, J. R., Edwards, R., Kok, G. L., Flanner, M. G., Zender, C. S., Saltzman, E.
734 S., Banta, J. R., Pasteris, D. R., Carter, M. M., and Kahl, J. D. W.: 20th-century
735 industrial black carbon emissions altered Arctic climate forcing, Science, 317,
736 1381–1384, doi:10.1126/science.1144856, 2007.

737 Ming, J., Cachier, H., Xiao, C., Qin, D., Kang, S., Hou, S., and Xu, J.: Black carbon
738 record based on a shallow Himalayan ice core and its climatic implications, Atmos.
739 Chem. Phys., 8, 1343–1352, doi:10.5194/acp-8-1343-2008, 2008.

740 Nair, V. S., Babu, S. S., Moorthy, K. K., Sharma, A. K., Marinoni, A., and Ajai: Black
741 carbon aerosols over the Himalayas: Direct and surface albedo forcing, Tellus B,
742 65, 19738, doi:10.3402/tellusb.v65i0.19738, 2013.

743 Painter, T. H., Seidel, F. C., Bryant, A. C., McKenzie Skiles, S., and Rittger, K.:
744 Imaging spectroscopy of albedo and radiative forcing by light-absorbing
745 impurities in mountain snow, J. Geophys. Res. Atmos., 118, 9511–9523,
746 doi:10.1002/jgrd.50520, 2013.

747 Parungo, F., Nagamoto, C., Zhou, M.-Y., Hansen, A. D.A., and Harris, J.: Aeolian
748 transport of aerosol black carbon from Aeolian transport of aerosol black carbon
749 from China to the ocean, Atmos. Environ., 28, 3251–3260, 1994.

750 Petr Chylek, V. R. and Srivastava, V.: Albedo of soot-contaminated snow, J. Geophys.
751 Res., 88, 10837–10843, 1983.

752 Petzold, A., Ogren, J. A., Fiebig, M., Laj, P., Li, S.-M., Baltensperger, U.,
753 Holzer-Popp, T., Kinne, S., Pappalardo, G., Sugimoto, N., Wehrli, C.,
754 Wiedensohler, A., and Zhang, X.-Y.: Recommendations for reporting "black
755 carbon" measurements, Atmos. Chem. Phys., 13, 8365–8379,
756 doi:10.5194/acp-13-8365-2013, 2013.

757 Ramanathan, V., Crutzen, P. J., Kiehl, J. T., and Rosenfeld, D.: Aerosols, climate, and
758 the hydrological cycle, Science, 294, 2119–2124, 2001.

759 Rasch, P. J., Mahowald, N. M., and Eaton, B. E.: Representations of transport,
760 convection, and the hydrologic cycle in chemical transport models: Implications
761 for the modeling of short-lived and soluble species, J. Geophys. Res., 102,
762 28,127–28,138, 1997.

763 Schmale, J., Flanner, M., Kang, S., Sprenger, M., Zhang, Q., Guo, J., Li, Y.,
764 Schwikowski, M., and Farinotti, D.: Modulation of snow reflectance and
765 snowmelt from Central Asian glaciers by anthropogenic black carbon, Sci. Rep., 7,
766 40501, doi:10.1038/srep40501, 2017.

767 Schwarz, J. P., Gao, R. S., Fahey, D. W., Thomson, D. S., Watts, L. A., Wilson, J. C.,
768 Reeves, J. M., Darbeheshti, M., Baumgardner, D. G., Kok, G. L., Chung, S. H.,
769 Schulz, M., Hendricks, J., Lauer, A., Krämer, B., Slowik, J. G., Rosenlof, K. H.,
770 Thompson, T. L., Langford, A. O., Loewenstein, M., and Aikin, K. C.:
771 Single-particle measurements of midlatitude black carbon and light-scattering
772 aerosols from the boundary layer to the lower stratosphere, J. Geophys. Res., 111,
773 2845, doi:10.1029/2006JD007076, 2006.

带格式的: 字体: Times New Roman, 小四, 无下划线, 字体颜色: 自动设置

带格式的: 字体: Times New Roman, 小四

带格式的: 字体: Times New Roman, 小四, 无下划线, 字体颜色: 自动设置

带格式的: 字体: Times New Roman, 小四

带格式的: 字体: Times New Roman, 小四, 无下划线, 字体颜色: 自动设置

带格式的: 字体: Times New Roman, 小四

带格式的: 字体: Times New Roman, 小四, 无下划线, 字体颜色: 自动设置

带格式的: 字体: Times New Roman, 小四

带格式的: 字体: Times New Roman, 小四, 无下划线, 字体颜色: 自动设置

带格式的: 字体: Times New Roman, 小四

带格式的: 字体: Times New Roman, 小四, 无下划线, 字体颜色: 自动设置

带格式的: 字体: Times New Roman, 小四

带格式的: 字体: Times New Roman, 小四, 无下划线, 字体颜色: 自动设置

带格式的: 字体: Times New Roman, 小四

带格式的: 字体: Times New Roman, 小四, 无下划线, 字体颜色: 自动设置

带格式的: 字体: Times New Roman, 小四

带格式的: 字体: Times New Roman, 小四, 无下划线, 字体颜色: 自动设置

带格式的: 字体: Times New Roman, 小四

带格式的: 字体: Times New Roman, 小四, 无下划线, 字体颜色: 自动设置

带格式的: 字体: Times New Roman, 小四

带格式的: 字体: Times New Roman, 小四

774 [Tie, X. X., Madronich, S., Walters, S., Edwards, D. P., Ginoux, P., Mahowald, N.,](#)
775 [Zhang, R. Y., Lou, C., and Brasseur, G.:](#) Assessment of the global impact of
776 [aerosols on tropospheric oxidants, *J. Geophys. Res.*, 110, 13,791,](#)
777 [doi:10.1029/2004JD005359, 2005.](#)

778 [Wang, M., Xu, B., Cao, J., Tie, X., Wang, H., Zhang, R., Qian, Y., Rasch, P. J., Zhao,](#)
779 [S., Wu, G., Zhao, H., Joswiak, D. R., Li, J., and Xie, Y.:](#) Carbonaceous aerosols
780 [recorded in a southeastern Tibetan glacier: Analysis of temporal variations and](#)
781 [model estimates of sources and radiative forcing, *Atmos. Chem. Phys.*, 15,](#)
782 [1191–1204, doi:10.5194/acp-15-1191-2015, 2015a.](#)

783 [Wang, M., Xu, B. Q., Kaspari, S. D., Gleixner, G., Schwab, V. F., Zhao, H. B., Wang,](#)
784 [H. L., and Yao, P.:](#) Century-long record of black carbon in an ice core from the
785 [Eastern Pamirs: Estimated contributions from biomass burning, *Atmos. Environ.*,](#)
786 [115, 79–88, doi:10.1016/j.atmosenv.2015.05.034, 2015b.](#)

787 [Warren, S. G. and Wiscombe, W. J.:](#) A Model for the Spectral Albedo of Snow. II:
788 [Snow Containing Atmospheric Aerosols, *J. Atmos. Sci.*, 37, 2734–2745,](#)
789 [doi:10.1175/1520-0469\(1980\)037<2734:AMFTSA>2.0.CO;2, 1980.](#)

790 [Wendl, I. A., Menking, J. A., Färber, R., Gysel, M., Kaspari, S. D., Laborde, M. J. G.,](#)
791 [and Schwikowski, M.:](#) Optimized method for black carbon analysis in ice and
792 [snow using the Single Particle Soot Photometer, *Atmos. Meas. Tech.*, 7,](#)
793 [2667–2681, doi:10.5194/amt-7-2667-2014, 2014.](#)

794 [Wiscombe, W. J. and Warren, S. G.:](#) A Model for the Spectral Albedo of Snow. I: Pure
795 [Snow, *J. Atmos. Sci.*, 37, 2712–2733,](#)
796 [doi:10.1175/1520-0469\(1980\)037<2712:AMFTSA>2.0.CO;2, 1980.](#)

797 [Wu, G. J., Yao, T. D., Xu, B. Q., Li, Z., Tian, L. D., Duan, K. Q., and Wen, L. K.:](#)
798 [Grain size record of microparticles in the Muztagata ice core, *Sci. China Ser. D*, 49,](#)
799 [10–17, doi:10.1007/s11430-004-5093-5, 2006.](#)

800 [Wu, G. J., Yao, T. D., Xu, B. Q., Tian, L. D., Li, Z., and Duan, K. Q.:](#) Seasonal
801 [variations of dust record in the Muztagata ice cores, *Sci. Bull.*, 53, 2506–2512,](#)
802 [doi:10.1007/s11434-008-0197-5, 2008.](#)

803 [Wu, T. and Qian, Z.:](#) The relation between the Tibetan winter snow and the Asian
804 [summer monsoon and rainfall: an observational investigation, *Journal of Climate*,](#)
805 [16, 2038–2051, 2003.](#)

806 [Xu, B., Cao, J., Hansen, J., Yao, T., Joswia, D. R., Wang, N., Wu, G., Wang, M., Zhao,](#)
807 [H., Yang, W., Liu, X., and He, J.:](#) Black soot and the survival of Tibetan glaciers, *P.*
808 [Natl. Acad. Sci. USA, 106, 22114–22118, doi:10.1073/pnas.0910444106, 2009a.](#)

809 [Xu, B. Q., Wang, M., Joswiak, D. R., Cao, J. J., Yao, T. D., Wu, G. J., Yang, W., and](#)
810 [Zhao, H. B.:](#) Deposition of anthropogenic aerosols in a southeastern Tibetan
811 [glacier, *J. Geophys. Res.*, 114, 9185, doi:10.1029/2008JD011510, 2009b.](#)

812 [Yasunari, T. J., Bonasoni, P., Laj, P., Fujita, K., Vuillermoz, E., Marinoni, A.,](#)
813 [Cristofanelli, P., Duchi, R., Tartari, G., and Lau, K.-M.:](#) Estimated impact of black
814 [carbon deposition during pre-monsoon season from Nepal Climate Observatory –](#)
815 [Pyramid data and snow albedo changes over Himalayan glaciers, *Atmos. Chem.*](#)
816 [Phys., 10, 6603–6615, doi:10.5194/acp-10-6603-2010, 2010.](#)

817 [Yasunari, T. J., Tan, Q., Lau, K.-M., Bonasoni, P., Marinoni, A., Laj, P., Ménégoz, M.,](#)

带格式的: 字体: Times New Roman, 小四, 无下划线, 字体颜色: 自动设置

带格式的: 字体: Times New Roman, 小四

带格式的: 字体: Times New Roman, 小四, 无下划线, 字体颜色: 自动设置

带格式的: 字体: Times New Roman, 小四

带格式的: 字体: Times New Roman, 小四, 无下划线, 字体颜色: 自动设置

带格式的: 字体: Times New Roman, 小四

带格式的: 字体: Times New Roman, 小四, 无下划线, 字体颜色: 自动设置

带格式的: 字体: Times New Roman, 小四

带格式的: 字体: Times New Roman, 小四, 无下划线, 字体颜色: 自动设置

带格式的: 字体: Times New Roman, 小四

带格式的: 字体: Times New Roman, 小四, 无下划线, 字体颜色: 自动设置

带格式的: 字体: Times New Roman, 小四

带格式的: 字体: Times New Roman, 小四, 无下划线, 字体颜色: 自动设置

带格式的: 字体: Times New Roman, 小四

带格式的: 字体: Times New Roman, 小四, 无下划线, 字体颜色: 自动设置

带格式的: 字体: Times New Roman, 小四

带格式的: 字体: Times New Roman, 小四, 无下划线, 字体颜色: 自动设置

带格式的: 字体: Times New Roman, 小四

带格式的: 字体: Times New Roman, 小四, 无下划线, 字体颜色: 自动设置

带格式的: 字体: Times New Roman, 小四

带格式的: 字体: Times New Roman, 小四, 无下划线, 字体颜色: 自动设置

带格式的: 字体: Times New Roman, 小四

带格式的: 字体: Times New Roman, 小四, 无下划线, 字体颜色: 自动设置

带格式的: 字体: Times New Roman, 小四

带格式的

818 Takemura, T., and Chin, M.: Estimated range of black carbon dry deposition and
819 the related snow albedo reduction over Himalayan glaciers during dry
820 pre-monsoon periods, Atmos. Environ., 78, 259–267,
821 doi:10.1016/j.atmosenv.2012.03.031, 2013.
822 Zhang, G. J. and McFarlane, N. A.: Sensitivity of climate simulations to the
823 parameterization of cumulus convection in the Canadian climate centre general
824 circulation model, Atmos. Ocean, 33, 407–446,
825 doi:10.1080/07055900.1995.9649539, 1995.
826 Zhao, H. B., Xu, B. Q., Yao, T. D., Tian, L. D., and Li, Z.: Records of sulfate and
827 nitrate in an ice core from Mount Muztagata, central Asia, J. Geophys. Res., 116,
828 275, doi:10.1029/2011JD015735, 2011.
829 Zhao, Z., Cao, J., Shen, Z., Xu, B., Zhu, C., Chen, L.-W. A., Su, X., Liu, S., Han, Y.,
830 Wang, G., and Ho, K.: Aerosol particles at a high-altitude site on the Southeast
831 Tibetan Plateau, China: Implications for pollution transport from South Asia, J.
832 Geophys. Res. Atmos., 118, 11,360-11,375, doi:10.1002/jgrd.50599, 2013.
833
834

带格式的: 字体: Times New Roman, 小四

带格式的: 字体: Times New Roman, 小四, 无下划线, 字体颜色: 自动设置

带格式的: 字体: Times New Roman, 小四

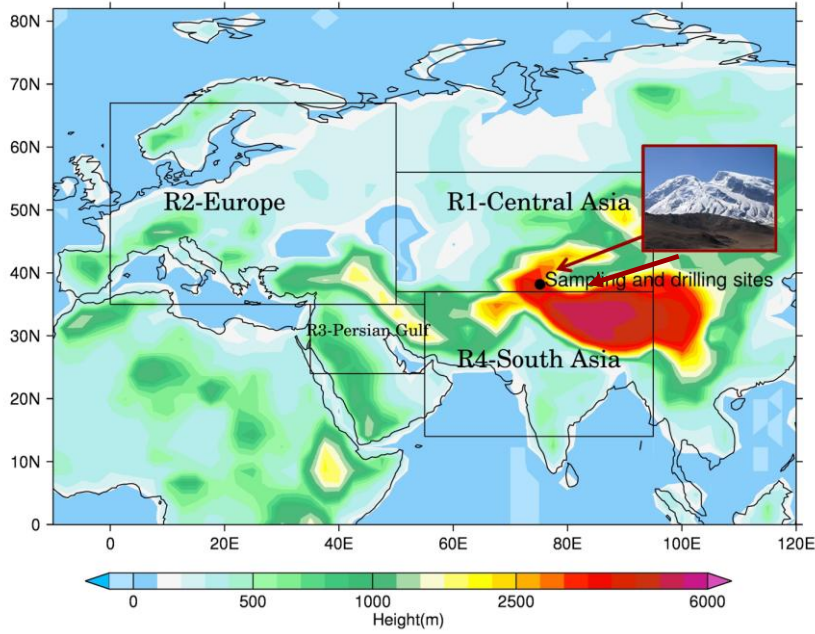
带格式的: 字体: Times New Roman, 小四, 无下划线, 字体颜色: 自动设置

带格式的: 字体: Times New Roman, 小四

带格式的: 字体: Times New Roman, 小四, 无下划线, 字体颜色: 自动设置

带格式的: 字体: Times New Roman, 小四

835



带格式的: 字体: (默认) Times New Roman, 10 磅, 无下划线, 字体颜色: 文字 1

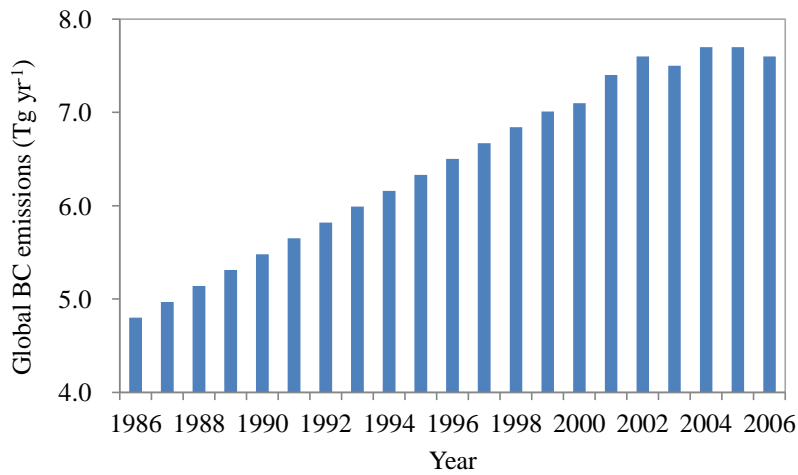
836



带格式的: 字体: (默认) Times New Roman, 10 磅, 无下划线, 字体颜色: 文字 1

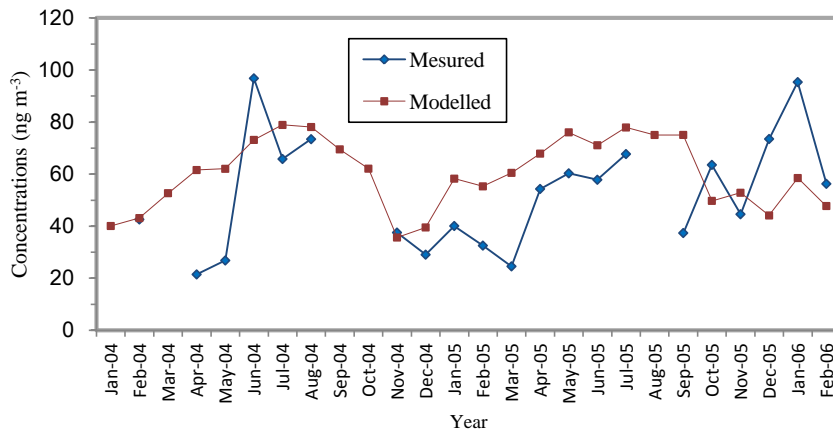
837

838 Fig 1. The Muztagh Ata measurement site (indicated by the red dot), and the surrounding BC source areas
839 (R1-Central Asia region; R2-European region; R3-Persian Gulf region; and R4-South Asia region).



840

841 Fig 2. The trend of global BC emission (Tg/yr) from 1986 to 2006 used in this study



842

843

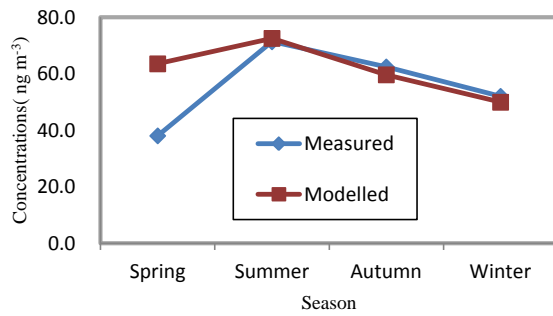
Fig 3a. Comparison of calculated (red) and measured (blue) monthly mean BC concentrations at the surface level during Jan. 2004 to Feb. 2006 measured by the Cold and Arid Regions Environmental and Engineering Institute, Chinese Academy of Sciences.

844

845

846

847



848

849

Fig 3b. Comparison of calculated (red) and measured (blue) seasonal variation during Jan. 2004 to Feb. 2006. Spring includes March, April and May in 2004 and 2005. Summer includes June, July and August in 2004, 2005; Autumn includes September, October and November in 2004, 2005; Winter includes December, January and February of 2004, 2005 and January, February in 2006.

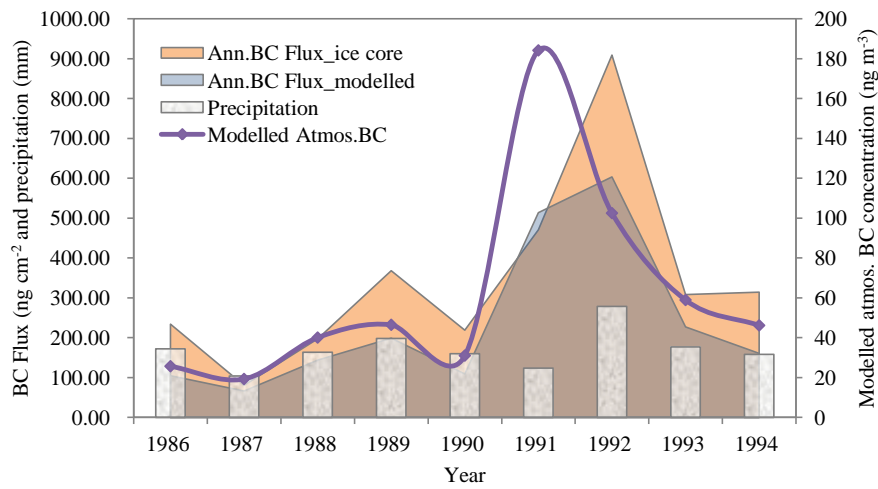
850

851

852

853

854



855

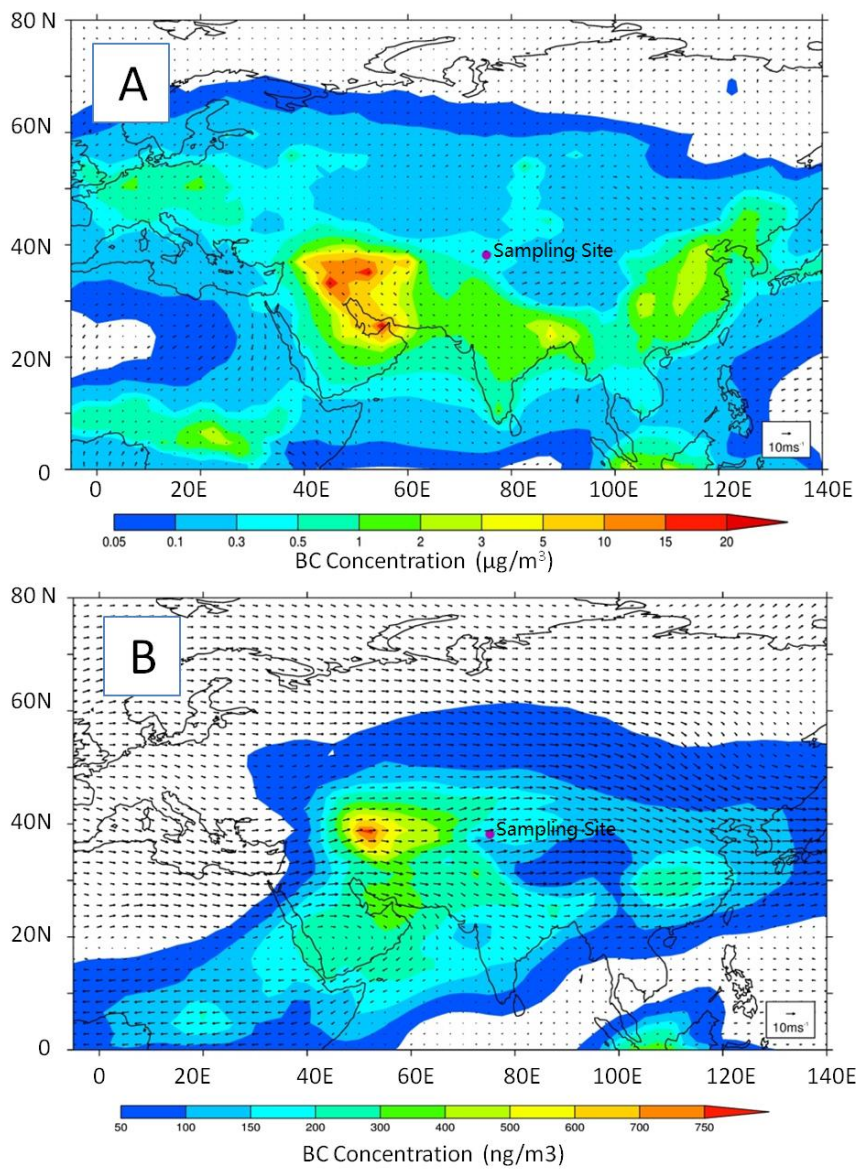
856 **Fig 4. Comparison of measured annual BC deposition flux with the model calculation between ice core and**
 857 **simulation, as well as the modelled atmospheric BC concentration and precipitation used for BC deposition**
 858 **flux calculation**

859



860

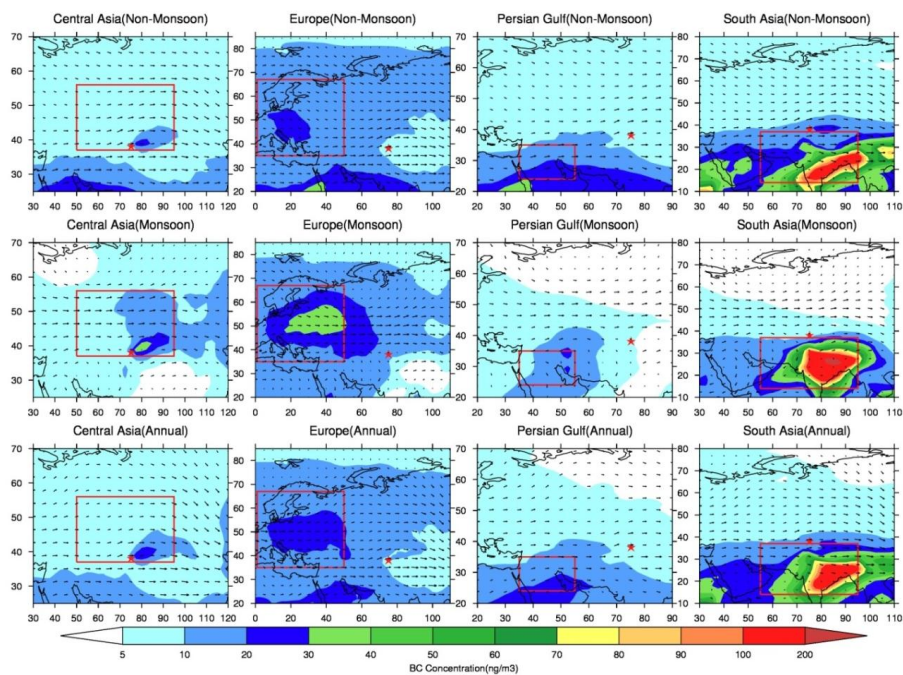
861 **Fig 5. The image of the fires in Kuwait during 1991. It shows the intensive fires and the raise up of plume**
 862 **due to the heat buoyance. The lower panel shows the fires were transported to east due to western winds.**



带格式的：居中，缩进：首行缩进：0 厘米

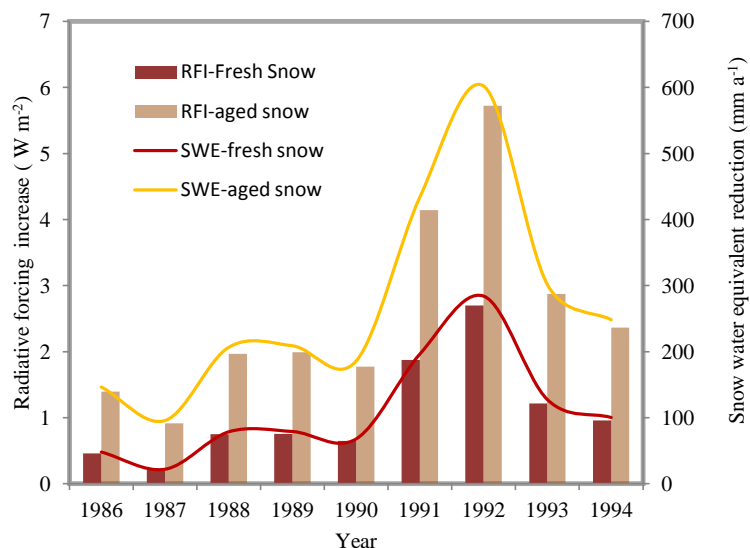
863
864
865
866
867

Fig. 6. The calculated horizontal distributions of BC concentrations ($\mu\text{g m}^{-3}$) at the surface (A) and the concentrations (ng m^{-3}) at 5 km above the surface (B) [in Kuwait during 1991](#). The wind direction and speed are indicated by black arrows.



868
 869
 870
 871
 872
 873
 874
 875
 876

Fig 7. The calculated spatial BC distributions due to individual BC from the four source regions (Central Asia, Europe, Persian Gulf and South Asia) above 5 km above the surface during different periods, i.e., monsoon (June-September), non-monsoon (October-May), and annual mean in 1993. The red star is where the study site of Muztagh Ata located. The red boxes indicate the boundary of the four source regions.



877

878 **Fig 8. Estimated the effects of BC containments on annual mean radiative forcing increase (RFI) (W/m^2)**
 879 **and snow water equivalent (SWE) reduction (mm/a), under fresh snow assumption (purple line and bars)**
 880 **and aged snow assumption (yellow line and bars).**

881

882

883 **Table 1. Source regions and corresponding fractional contributions to atmospheric BC concentrations at the**
 884 **Muztagh Ata site in monsoon, non-monsoon and all months during 1993**

885

	Source regions	Latitude	Longitude	Summer monsoon (June-September)	Non-monsoon (October-May)	Annual
R1	Central Asia	37-56 °N	50-95 °E	43.9%	18.1%	26.7%
R2	Europe	35-67 °N	0-50 °E	26.6%	11.5%	16.5%
R3	Persian Gulf	24-35 °N	35-55 °E	9.4%	12.1%	11.2%
R4	South Asia	14-37 °N	55-95 °E	7.3%	33.7%	24.9%
	Others	NA	NA	7.9%	6.2%	6.8%

886

887

888

889

890